A Dual-Topology Wireless Power Transfer System with Constant Current or Constant Voltage Output for Battery Charging Application

Mojtaba Khalilian[1] and Paolo Guglielmi[2]

[1,2] *Department of Energy, Politecnico di Torino*
Corso Duca degli Abruzzi 24, 10129, Turin, Italy

ORCIDs: (0000-0002-0984-9153)[1], (0000-0002-5452-8869)[2]

Abstract

In this paper, a novel dual-topology wireless power transfer system for the battery charging application is presented. The power circuit configuration is composed of Series-Series (SS) and S-LCL topologies. The SS compensation topology provides load independent current output and S-LCL compensation topology provides load independent voltage output for the process of the battery charging. The transmitter H-bridge converter operates in fixed frequency and with full square wave in its output. The transfer from the constant current mode to constant voltage mode is performed through the switching in the receiver side and without the communication path between the transmitter and receiver. The theoretical analysis and design considerations are presented in this paper. The simulation results show good performance of the proposed battery charger along with good compatibility with the theoretical analysis.

Keywords: Battery charger, compensation topology, load-independent current output, load-independent voltage output, wireless power transmission.

I. INTRODUCTION

Wireless power transfer (WPT) concept is the transmission of the power from the source to the load wirelessly and without any connection using inductive coupling. The elimination of the electrical connection provides some benefits such as increase of safety, lifetime and reliability. Recently, WPT systems are widely used in many applications such as battery charger of electric vehicles, cellphones and medical devices [1]-[3].

The lithium-ion batteries are widely used in many applications. The charging process of a lithium-ion battery is composed of the constant current (CC) step and constant voltage (CV) step [4]. First, the battery is charged with the CC until the battery voltage reaches a certain value and then the battery is charged in CV mode until the charging current of it reaches nearly zero. During the charging process, the battery equivalent resistance changes considerably. Thus, the control must be able to maintain the battery current or the battery voltage constant independent of these load variations.

Different works have been done to control the charging process of a battery. These techniques are classified into control strategies [5]-[14] and compensation topologies [15]-[24]. Depending on where the control is applied, the introduced control strategies are classified into three types: transmitter side control [5]-[10], receiver side control [11] and dual-side control

[12]-[14]. The output current and voltage of the battery can be regulated from the transmitter side by H-bridge converter with fixed frequency operation using phase shift modulation [5], [6] or variable frequency control [7], [8]. With phase shift modulation control in the transmitter side for control of the output current or voltage, the soft switching for the H-bridge converter cannot be achieved in different load conditions. In [8], the CC and CV outputs are achieved through the operation of the transmitter converter at two different frequencies. However, the maximum efficiency cannot be obtained during the CV operating mode since the system does not operate at resonant frequency. In [9], a separate DC-DC converter is placed in the transmitter side and before the H-bridge converter in order to control the output of the WPT system. In receiver side control, the output current or voltage is regulated from the receiver side using a DC-DC converter [11]. In dual side control [12]-[14], the output power or voltage is controlled using power electronics in both sides of the system. In [13], an active rectifier is employed instead of the diode-bridge and DC-DC converter in order to build a bidirectional power transfer system. The disadvantage of the transmitter side control and dual side control is that the current and voltage of the battery are required to be sent to the transmitter side. However, adding the communication link between the transmitter and receiver makes the control complicate, reduces the reliability and increases the size and cost.

Different compensation topologies such as basic compensation topologies and high order compensation topologies have be presented in the literature [15]-[16]. Considering the supply voltage constant, each topology has a specific CC or CV characteristic at ZPA (zero phase angle) frequency. In order to provide both CC and CV characteristics at the same time, one idea is the construction of a hybrid topology and proper switching between them [17]-[24]. In [17], realization of the CC and CV modes is proposed with a dual topology WPT system composed of series-series (SS) and series-parallel (SP) topologies. However, this system is composed of a center tap transformer. Two hybrid topologies, one SS and parallel-series (PS) and the other SP and parallel-parallel (PP) compensations, are proposed in [18] for the CC and CV charging of the battery. In [18]-[20] communication path for the data exchange between the two sides of the system is necessary.

In this paper, a new WPT system for the charging of a battery is proposed. The CC and CV method are provided with a dual-topology system. The advantage of the proposed method is that the charging process control is taken place from the receiver side and there is no need for the communication link between the transmitter and receiver sides. This simplifies the control

and reduces the size and cost of the system. The theoretical operation of the proposed topology is presented in this paper. Finally, the proposed topology with charging current of 2 A and output voltage of 100 V is designed and simulated in order to validate the theoretical analysis.

II. FUNDAMENTAL ANALYSIS

II.I Battery Charge Profile

Lithium-ion batteries are suitable for different applications such as cell phones, electric vehicles, etc. The charging process of the battery consists of two main modes: first, charging with CC until the battery voltage reaches a certain value and second, charging with CV until the charging current of the battery reaches almost zero. The charging process of a battery is shown in Fig. 1. In the mode of constant current charging, the battery is charged by maintaining its current constant. There is a nearly linear increase of the battery voltage in the constant current charging period. At the end of this stage, the battery voltage is in its peak value. At this point, constant voltage charging mode starts. During this stage, the voltage of the battery is maintained constant and the charging current reduces. Thus, both constant current source and constant voltage source operations are necessary in battery charging application.
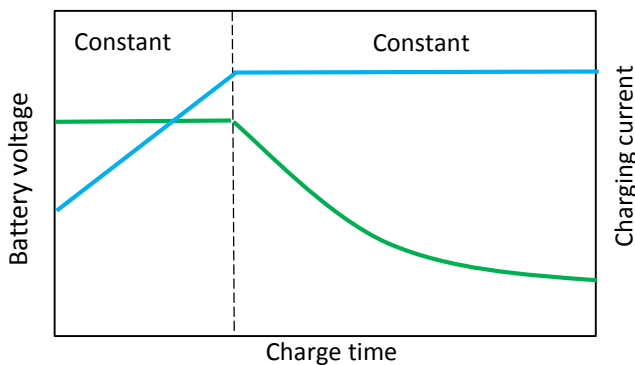

Fig. 1. Charging process for a lithium-ion battery

II.II SS compensation circuit with CC output

The equivalent circuit of a WPT system with the SS compensated circuit is presented in Fig. 2. L_1 and L_2 are self-inductances of the transmitter and receiver coils and M is mutual inductance. R_1 and R_2 are the resistances of the transmitter and receiver coils, respectively. Furthermore, C_1 and C_2 are the compensation capacitors of the transmitter and receiver, respectively. The resistance R_{ac} is the equivalent load resistance. By writing the voltage equations for the two sides of the system, the following equation set is obtained:

$$\begin{cases} V_1 = \left(R_1 + j\omega L_1 + \dfrac{1}{j\omega C_1}\right)i_1 - j\omega M i_2 \\ j\omega M i_1 = \left(R_2 + j\omega L_2 + \dfrac{1}{j\omega C_2}\right)i_2 + R_{ac} i_2 \end{cases} \quad (1)$$

The values resonant capacitors are designed in order to compensate the inductance of the coil in resonant frequency ω_0 as follows:
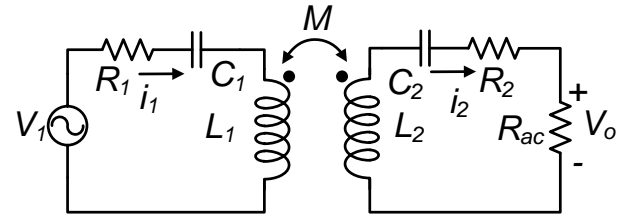

Fig. 2. Equivalent circuit of WPT system with SS compensation

$$\omega_0 = \frac{1}{\sqrt{L_1 C_1}} = \frac{1}{\sqrt{L_2 C_2}} \quad (2)$$

By rewriting (1) and considering that the system operates at resonant frequency according to (2), the current of the receiver is calculated as follows:

$$i_2 = \frac{j\omega_0 M V_1}{R_1(R_2 + R_{ac}) + \omega_0^2 M^2} \quad (3)$$

Mostly in design of the WPT systems, $\omega_0^2 M^2 \gg R_1$ and thus, the receiver current is approximately constant with the variation of the load. By neglecting the resistances of the transmitter and receiver coil, (3) can be simplified as follows:

$$i_2 = \frac{V_1}{j\omega_0 M} \quad (4)$$

According the (4), the current of the receiver is load independent when the switching frequency is equal to resonant frequency and the mutual inductance and the transmitter voltage are maintained constant.

II.III S-LCL compensation circuit with CV output

The equivalent circuit of the WPT system with S-LCL compensation is presented in Fig. 3. In the transmitter side, a series compensation is employed. In the receiver side, additional the inductor L_3 is added to the circuit to build an LCL compensation circuit.
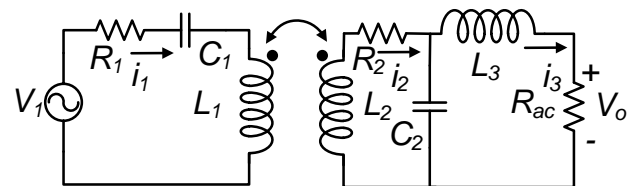

Fig. 3. Equivalent circuit of the WPT system with S-LCL compensation

By writing the Kirchhoff's voltage law for the transmitter and receiver sides, the following equations set is obtained:

$$\begin{cases} V_1 = \left(R_1 + j\omega L_1 + \dfrac{1}{j\omega C_1}\right)i_1 - j\omega M i_2 \\ j\omega M i_1 = \left(R_2 + j\omega L_2 + \dfrac{1}{j\omega C_2}\right)i_2 - \dfrac{1}{j\omega C_2}i_3 \\ V_o = \dfrac{1}{j\omega C_2}i_2 - \left(j\omega L_3 + \dfrac{1}{j\omega C_2}\right)i_3 \end{cases} \quad (5)$$
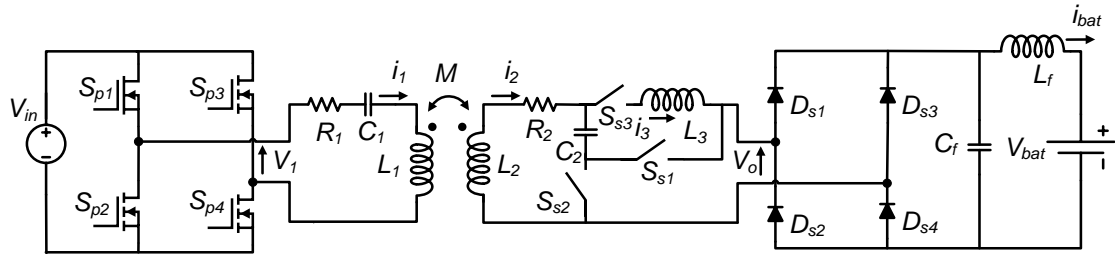
Fig. 4. Power circuit configuration of the proposed dual-topology WPT system

The series compensation is employed in the transmitter side and the frequency of the transmitter is equal to the resonant frequency of the C_1 and L_1. Similar to SS compensation circuit, the current at the input of the LCL is approximately constant. In order to have the load independent output voltage, the value of the L_2 and C_3 must be selected according to the following equation:

$$\omega_0 = \frac{1}{\sqrt{L_3 C_2}} \qquad (6)$$

By writing the equation for the impedance of the receiver Z_R, the following equation is obtained:

$$Z_R = \frac{R_{ac}\left(\frac{1}{j\omega C_2} + j\omega L_2\right) + \frac{1}{\omega^2 C_2{}^2}}{R_{ac}} \qquad (7)$$

In order to make the impedance of the receiver purely resistive, the following equation must be justified:

$$\omega_0 = \frac{1}{\sqrt{L_2 C_2}} \qquad (8)$$

Thus, the impedance of the receiver at the resonant frequency is obtained as:

$$Z_R = \frac{\omega_0{}^2 L_2{}^2}{R_{ac}} \qquad (9)$$

Since in the transmitter side a series compensation is employed, by making the impedance of the receiver resistive, the total impedance seen from the input source (Z_{in}) will be resistive as follows:

$$Z_{in} = \frac{M^2 R_{ac}}{L_2{}^2} \qquad (10)$$

Since Z_{in} is purely resistive, the zero phase angle (ZPA) for the transmitter converter can be achieved. By putting (6) and (8) into (5) and rewriting it, the output voltage equation of the S-LCL compensation circuit is calculated as follows

$$V_o = \frac{L_3 M V_1 \omega_0{}^2 R_{ac}}{M^2 \omega_0{}^2 R_{ac} + R_1 R_2 R_{ac} + R_1 L_3{}^2 \omega_0{}^2} \qquad (11)$$

The value of $R_{ac} \gg R_1$ and thus, the receiver output voltage is approximately constant with the variation of the load. By neglecting the resistances of the transmitter and receiver coil, the output voltage equation is simplified as

$$V_o = \frac{L_3 V_1}{M} \qquad (12)$$

It can be seen from (12) that if the converter works at the resonant frequency, the output voltage is independent of the load. It is only depended on the input voltage, mutual inductance and inductor L_3. In conclusion, in order to have constant voltage at the output of the S-LCL converter accompanied with the ZPA at the transmitter side, the value of the resonant element at the receiver side must be designed according to $L_2 = L_3 = 1/\omega_0 C_2$.

III. DUAL-TOPOLOGY AS BATTERY CHARGER

The power circuit configuration of the proposed dual-topology WPT system is presented in Fig. 4. As shown in this figure, the transmitter and receiver coils are common for both topologies. Furthermore, only one resonant capacitor is employed in the receiver side for both topologies. The switching between the two topologies is performed with three switches in the receiver side and thus, there is no need for the communication link between the transmitter and receiver. The control is only based on the values of the battery voltage and current. The switches are needed to be AC switches to provide the bidirectional current in both CC and CV modes and can be realized for example by two anti-series MOSFET. During the CC mode, S_{s1} is on and S_{s2} and S_{s3} are off. Thus, C_2 becomes in series with L_2 and L_3 becomes disconnected. During the CV mode, by turning on S_{s2}, C_2 becomes in parallel with the receiver coil and by turning on S_{s3} and turning off S_{s2}, LCL circuit is constructed.

With fundamental harmonic analysis of the circuit, it is possible to model the effect of the H-bridge converter and diode rectifier. The output voltage of the H-bridge converter is a square wave and thus, the first harmonic of it can be expressed as

$$V_1 = \frac{2\sqrt{2}}{\pi} V_{in} \cos\left(\frac{\alpha}{2}\right) \qquad (13)$$

Where, α is the phase shift angle between the two legs of the H-bridge converter. It this paper it is considered that the output voltage of the H-bridge converter is a full square wave and α is equal to zero. Furthermore, the voltage waveform at the input of the diode rectifier is a square wave and in the similar way, the first harmonic of it is given by

$$V_o = \frac{2\sqrt{2}}{\pi} V_{bat} \qquad (14)$$

Also, the relation between the battery current and the current at the input of the rectifier is based on the following equation.

$$i_o = \frac{\pi\sqrt{2}}{4} i_{bat} \qquad (15)$$

The battery equivalent resistance (R_{bat}) is defined as the relation between the voltage and current of the battery. The relation between the R_{bat} and R_{ac} is calculated based on the following equation:

$$R_{bat} = \frac{V_{bat}}{i_{bat}} = \frac{\pi^2}{8} R_{ac} \qquad (16)$$

IV. DESIGN CONSIDERATIONS

The battery specification is 100 V and 2 A. The input DC voltage V_{in} is 50 VDC. The H-bridge converter works with the fixed switching frequency of 85 kHz. The output voltage of the H-bridge converter is a full square wave and the phase shift between the two legs of the converter is zero. Based on (13), V_1 is calculated 45 V. According to (14) and (15), the values of the V_o and i_o are calculated 90 V and 2.22 A, respectively. By defining the current of the receiver 2.22 A, the mutual inductance M is calculated 37.92 uH according to (4). In order to have the constant voltage of 100 V at the battery side for the S-LCL converter, the value of L_3 is designed 75.86 uH based on (12). After designing the value of L_3, the values of L_2 and C_2 can be calculated easily from (6) and (8). The value of L_2 and C_2 are designed 75.86 uH and 46.22 nF respectively. Considering the calculated values M and L_2, the value of L_1 is obtained from the finite element analysis simulation according to the design limitations such as size and shape of the coils and air gap between them.

One issue that must be considered in the design of the circuit is that the resistances of the transmitter and receiver coils affect the output voltage and current. In CC mode and according to (3), if the battery equivalent resistance increases, the output current decreases and the constant output operating is affected. The variation of the output current versus the battery equivalent resistance for two different values of R_1 and R_2 are shown in Fig. 5. As shown in this figure, If R_1 and R_2 increase, this variation will be greater. During the CV operating mode, if the battery equivalent resistance increases, according to (11), the output voltage will increase. The variation of the output voltage versus the battery equivalent resistance for two different values of R_1 and R_2 are shown in Fig. 6. As shown in this figure, by increasing the coil resistances, the output voltage variation increases. Thus, the transmitter and receiver must be designed with Litz wires and low ESR capacitors.
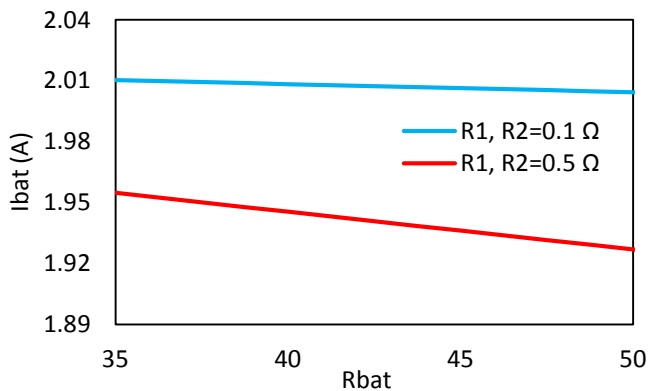

Fig. 5. Variations of the output current versus the battery equivalent resistance when battery charger works in CC mode
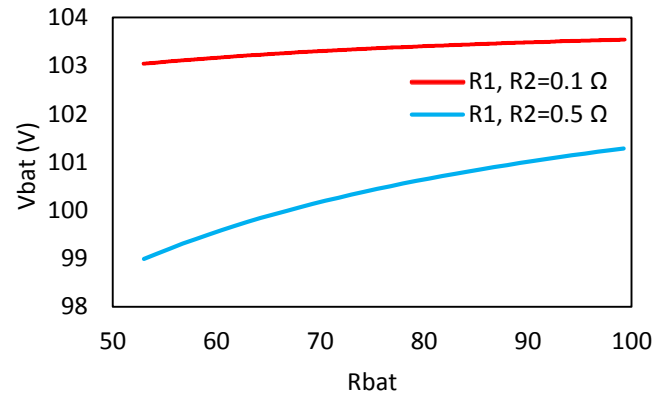

Fig. 6. Variations of the output voltage versus the battery equivalent resistance when battery charger works in CV mode
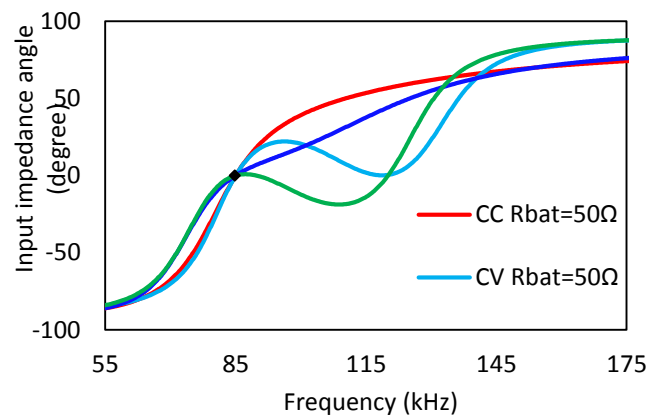

Fig. 7. Input impedance angle versus frequency for different R_{bat} and for different charging modes
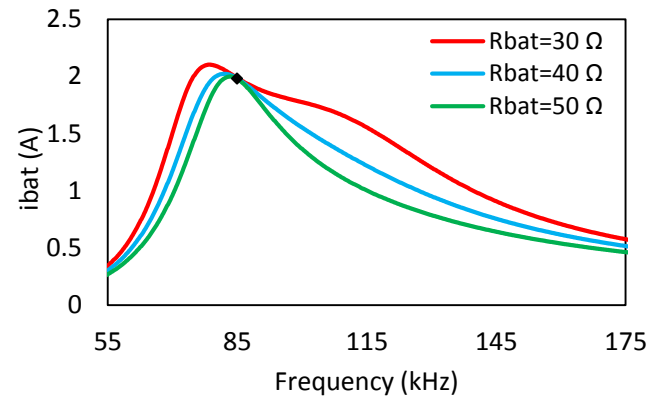

Fig. 8. Battery current versus frequency for different R_{bat} and in CC mode

Fig. 7 shows the input impedance angle versus frequency for different battery equivalent resistances for both charging modes. It can be seen from this figure that at resonant frequency of 85 kHz, the input impedance is purely resistive and the input impedance angle is zero. Thus, ZPA condition for the transmitter in both CC and CV mode can be achieved. The battery current versus switching frequency for different battery equivalent resistances in CC operating mode is presented in Fig. 8. It is clear that at resonant frequency, the battery current is independent of the load variations. Fig. 9 shows the battery voltage versus the switching frequency for different load

conditions when the battery charger is in CV mode. As shown in this figure, the battery voltage is constant independent of the load variations, when the system operates in resonant frequency.
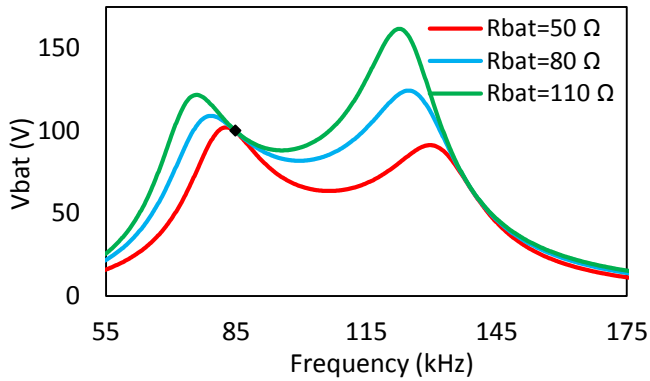

Fig. 9. Battery voltage versus frequency for different R_{bat} and in CV mode

V. CONTROL SCHEME

The control scheme of the battery charger is shown in Fig. 10. The battery charger is composed of three switches which must be switched properly in order to complete the charging process of the battery. The switches employed for the control are high frequency AC switches. According to the control scheme, the voltage of the battery is measured and compared with the reference voltage which is the voltage level that the control must change the charging mode from the CC to CV mode.
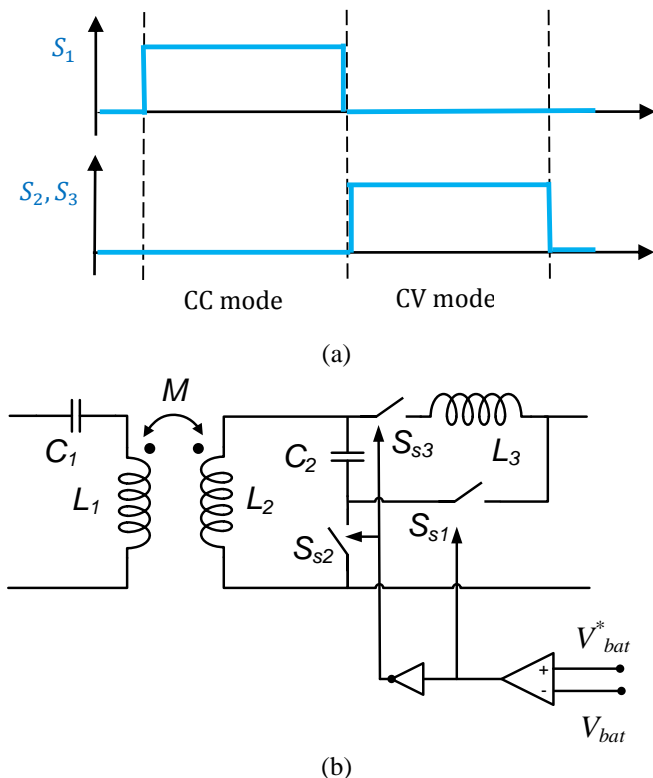

(a)

(b)

**Fig. 10.** Battery voltage versus frequency for different R_{bat} and in CV mode

At the beginning of the charging process, the voltage of the battery is lower than the reference voltage and thus, switch S_{s1} turns on and switches S_{s2} and S_{s3} turns off and the charging process in CC mode starts. The voltage of the battery start increasing. At the moment that the voltage of the battery reaches the maximum voltage level, switch S_{s1} turns off and switches S_{s2} and S_{s3} turn on. The charging mode, changes from the CC mode to CV mode and the current of the battery starts decreasing until it reaches approximately zero.

VI. SIMULATION RESULTS

In order to validate the theoretical analysis, the proposed battery charger with the output current of 2 A and output voltage of 100 V is built according to the parameters presented in TABLE I. The transmitter H-bridge converter operates in fixed frequency of 85 kHz. The transmitter current and voltage in CC mode with the battery equivalent resistance of 30 Ω are shown in Fig. 11(a). Furthermore, the current and voltage of the battery are illustrated in Fig. 11(b). As shown in this figure, the battery current is 2 A and the battery voltage is around 60 V. The current and voltage waveforms of the transmitter in CC mode and with the battery equivalent resistance of 50 Ω are presented in Fig. 12(a). Also, the battery voltage and current are shown in Fig. 12(b). It can be seen from this figure that the battery voltage is 100 V and the battery current is 2 A. During this mode, switch S_{s1} is on and switches S_{s2} and S_{s3} are off. During the CC mode, current of the battery is maintained constant at the level of 2 A when R_{bat} increases from 30 Ω to 50 Ω. The next charging mode of the battery is CV. This mode starts when the voltage of the battery reaches 100 V. At this moment, switch S_{s1} turns off and switches S_{s2} and S_{s3} turn on. Fig. 13(a) shows the current and voltage of the transmitter in CV charging mode and the battery equivalent resistance of 50 Ω. As shown in Fig 13(b), the current and voltage of the battery in R_{bat} equal to 50 Ω are 100 V and 2 A respectively. At this resistance, the values of the battery voltage and current for SS topology and S-LCL topology are equal. The current and voltage waveforms of the transmitter with R_{bat} of 90 Ω are presented in Fig. 14(a). Furthermore, the current and voltage of the battery is presented in Fig. 14 (b). The charging profile of the battery versus the battery equivalent resistance variations is shown in Fig. 15. It can be seen from this figure that the WPT system can provide both CC and CV modes when the battery equivalent resistance changes during the charging process.

Table 1. Specification and parameters of the WPT system

| Parameter	Value	Unit
Transmitter resistance, R_1	0.2	Ω
Transmitter inductance, L_1	200	μH
Transmitter capacitor, C_1	17.53	nF
Receiver resistance, R_2	0.2	Ω
Receiver inductances, L_2	75.86	μH
Receiver additional inductor, L_3	75.86	μH
Receiver capacitor, C_2	44.95	nF
Mutual inductance, M	37.92	μH
Input DC voltage, V_{in}	50	V
Battery current, i_{bat}	2	A
Battery voltage, V_{bat}	60-100	V
Switching frequency, f_0	85	kHz
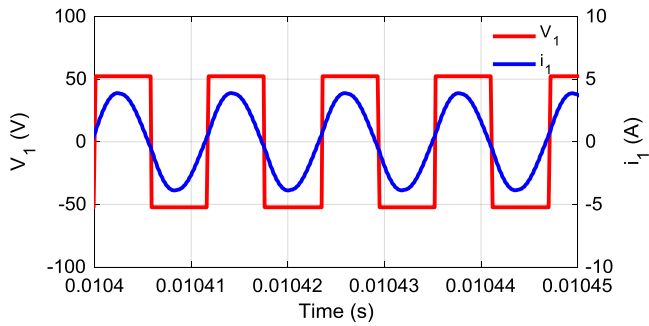
(a)
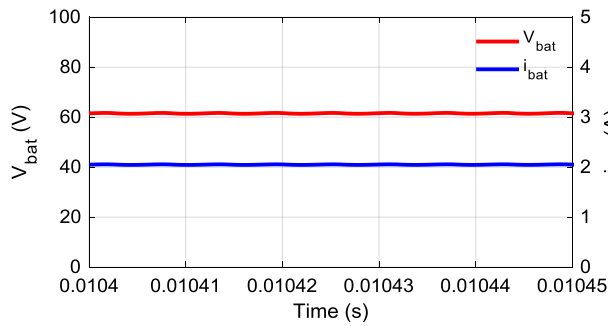
(b)

Fig. 11. Operation in CC mode with SS topology when R_{bat} is 30 Ω. (a) Voltage and cucurnt of the transmitter, (b) voltage and current of the battery
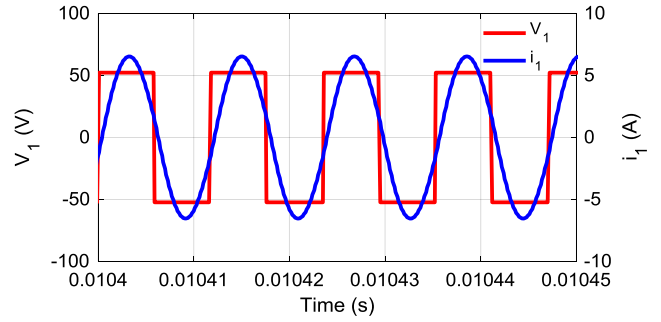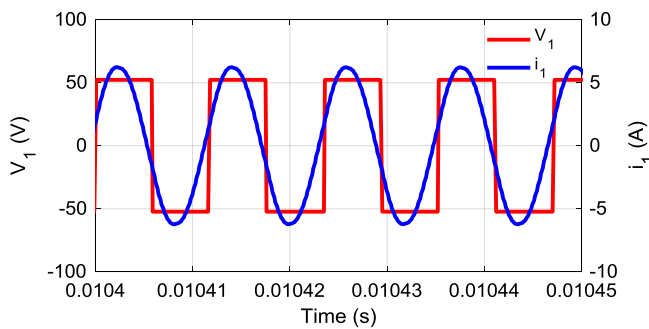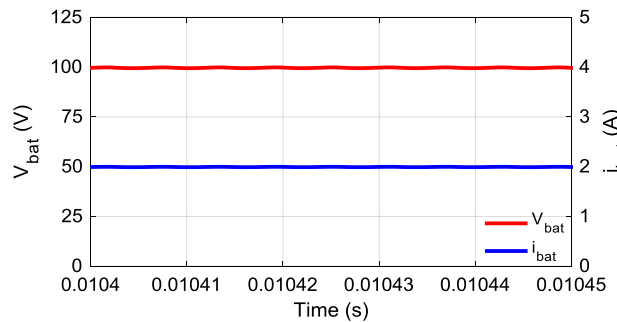

(a)
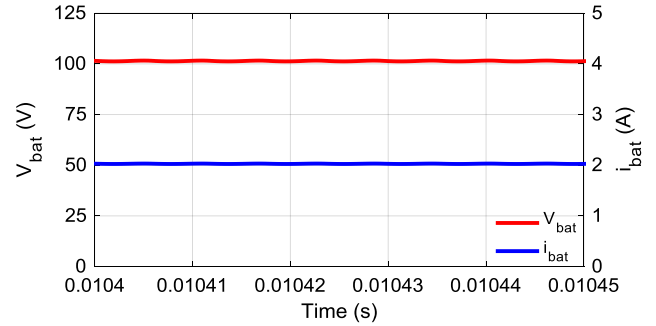
(b)

Fig. 13. Operation in CV mode with S-LCL topology when R_{bat} is 50 Ω. (a) Voltage and cucurnt of the transmitter, (b) voltage and current of the battery
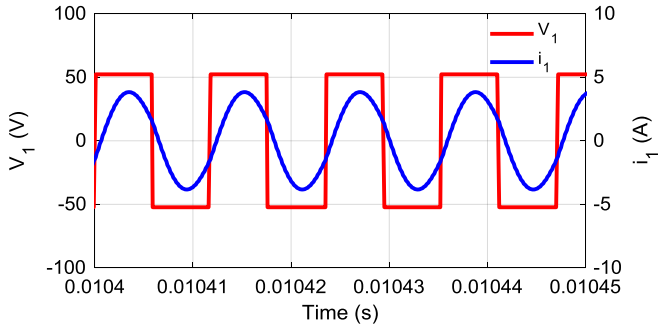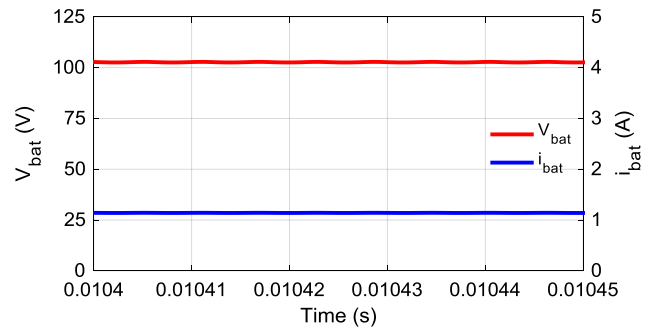

(a)

(b)

Fig. 12. Operation in CC mode with SS topology when R_{bat} is 50 Ω. (a) Voltage and cucurnt of the transmitter, (b) voltage and current of the battery

(a)

(b)

Fig. 14. Operation in CV mode with S-LCL topology when R_{bat} is 90 Ω. (a) voltage and cucurnt of transmitter, (b). voltage and current of battery
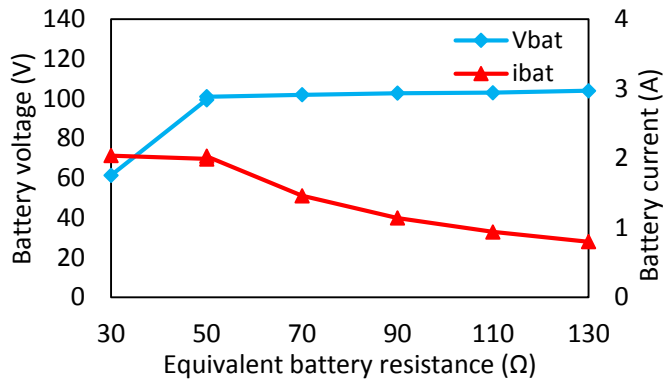
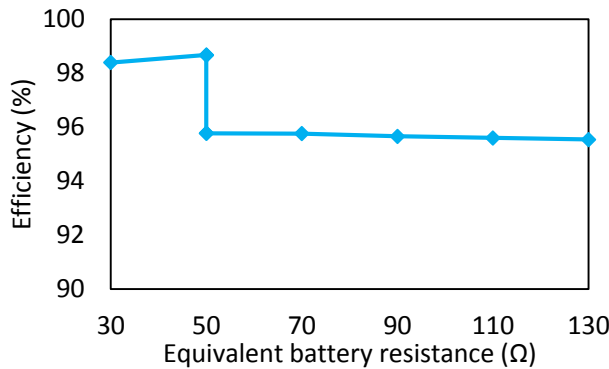**Fig. 15.** Charging profile of the battery during the charging process

Fig. 16. Efficiency during the charging process

The efficiency of the system versus the equivalent battery resistance is shown in Fig. 16. During the charging process in CC mode, the efficiency increases. At the R_{bat} equal to 50 Ω and with SS topology, the maximum efficiency for the system is obtained. When the topology is changed from SS to S-LCL, the efficiency reduces. This is due effect of the additional inductor's resistance. During the charging is CV mode and increase of the battery equivalent resistance, the efficiency reduces.

VII. CONCLUSION

In this paper, a new dual-topology WPT system for the battery charging application is proposed. The hybrid topology is composed of SS and S-LCL topology. The SS topology provides CC charging and S-LCL topology provides CV charging. The advantage of the proposed topology is that transmitter H-bridge converter operates at fixed switching frequency and phase shift angle between two legs of it is zero. It means that the H-bridge converter output voltage is a full square wave during the whole charging process Also, the WPT system operates in ZPA and thus, the efficiency can be improved. For the control of the charging process it is not necessary to send the parameters of the battery to the transmitter side. The lack of any communication link for data exchange makes the control and implementation simple. Furthermore, it is not necessary to add a DC-DC converter to the receiver side. The results obtained by the simulation validates the theoretical analysis.

REFERENCES

[1] W. Li, H. Zhao, S. Li, J. Deng, T. Kan, and C. C. Mi, "Integrated LCC Compensation Topology for Wireless Charger in Electric and Plug-in Electric Vehicles," *IEEE Trans. Ind. Electron.*, vol. 62, no. 7, pp. 4215– 4225, Jul. 2015.

[2] V. Cirimele, F. Freschi, and M. Mitolo, "Inductive power transfer for automotive applications: State-of-the-art and future trends," in *2016 IEEE Industry Applications Society Annual Meeting*, Portland, OR, USA, 2016, pp. 1–8.

[3] S. Y. Choi, B. W. Gu, S. Y. Jeong and C. T. Rim, "Advances in wireless power transfer systems for roadway-powered electric vehicles," *IEEE J. Emerg. Select. Topics Power Electron.*, vol. 3, no. 1, pp.18–36, 2015.

[4] A. Khaligh and Z. Li, "Battery, ultracapacitor, fuel cell, and hybrid energy storage systems for electric, hybrid electric, fuel cell, and plug-in hybrid electric vehicles: State of the art," *IEEE Trans. Veh. Technol.*, vol. 59, no. 6, pp. 2806–2814, Jul. 2010.

[5] C. Wang, C. Zhu, K. Song, G. Wei, S. Dong, R. Lu, "Primary-side control method in two-transmitter inductive wireless power transfer systems for dynamic wireless charging applications," In *Emerging Technologies: Wireless Power Transfer (WoW),* pp. 1-6, 2017.

[6] J. M. Miller, O. C. Onar and M. Chinthavali, "Primary-Side Power Flow Control of Wireless Power Transfer for Electricc Vehicle Charging," *IEEE Journal of Emerging and Selected Topics in Power Electron.*, vol. 3, no. 1, pp. 142-163, March, 2015.

[7] E. Gati, G. Kampitsis, and S. Manias, "Variable frequency controller for inductive power transfer in dynamic conditions," *IEEE Trans. Power Electron.*, vol. 32, no. 2, pp. 1684–1696, Feb. 2017.

[8] Z. Huang, S. Wong, and C. K. Tse, "Design methodology of a seriesseries inductive power transfer system for electric vehicle battery charger application," in *Proc. IEEE Energy Convers. Congr. Expo. ,* pp. 1778–1782, 2014.

[9] H. Li, J. Li, K. Wang, W. Chen, and X. Yang, "A maximum efficiency point tracking control scheme for wireless power transfer systems using magnetic resonant coupling," *IEEE Trans. Power Electron.*, vol. 30, no. 7, pp. 3998–4008, Aug. 2014.

[10] D. J. Thrimawithana and U. K. Madawala, "A primary side controller for inductive power transfer systems," *in Proc. IEEE Int. Conf. Ind. Electron.*, Viña del Mar, Chile, pp. 661–666, 2010.

[11] G. Lovison, T. Imura, and Y. Hori, "Secondary-side-only simultaneous power and efficiency control by online mutual inductance estimation for dynamic wireless power transfer," in *IECON 2016 - 42nd Annual*

Conference of the IEEE Industrial Electronics Society, pp. 4553- 4558, 2016.

[12]   R. Ruffo, M. Diana, V. Cirimele, M. Khalilian, A. La Ganga, and P. Guglielmi "Sensorless control of the charging process of a dynamic inductive power transfer system with interleaved nine-phase boost converter," *IEEE Trans. Ind. Electron*., 2018.

[13]   T. Diekhans and R. W. D. Doncker, "A dual-side controlled inductive power transfer system optimized for large coupling factor variations and partial load," *IEEE Trans. Power Electron*., vol. 30, no. 11, pp. 6320–6328, Nov. 2015.

[14]   H. H. Wu, A. Gilchrist, K. D. Sealy, and D. Bronson, "A high efficiency 5 kW inductive charger for EVs using dual side control*," IEEE Trans. Ind. Informat*., vol. 8, no. 3, pp. 585–595, Aug. 2012.

[15]   W. Zhang and C. C. Mi, "Compensation topologies for high power wireless power transfer systems*," IEEE Trans. Veh. Technol*., vol. PP, no. 99, pp. 1-10, Jul. 2015.

[16]   F. Liu, Y. Zhang K. Chen, Z. Zhao, L. Yuan, "A comparative study of load characteristics of resonance types in wireless transmission systems," in *Electromagnetic Compatibility (APEMC)*, pp. 203-206, 2016.

[17]   C. Auvigne, P. Germano, D. Ladas, and Y. Perriard, "A dual-topology ICPT applied to an electric vehicle battery charger," in *Proc. Int. Conf. Elect. Mach.*, Mar., 2012, pp. 2287–2292.

[18]   X. Qu, H. Han, S. C. Wong, C. K. Tse, and W. Chen, "Hybrid IPT topologies with constant current or constant voltage output for battery charging applications," *IEEE Trans. Power Electron.*, vol. 30, no. 11, pp. 6329–6337, Nov. 2015.

[19]   J.H. Lu, W.J. Li, B. Li, G.R Zhu, "Variable compensation network for achieving constant current or voltage output in IPT system," *Int. Conf. Industrial Informatics Computing Technology, Intelligent Technology, Industrial Information Integration (ICIICII)*, pp. 14–17, 2016.

[20]   R. Mai, R., Y. Chen, Y. Zhang, N. Yang, G. Cao, and Z. He, "Optimization of the passive components for an S-LCC topology-based WPT system for charging massive electric bicycles. *IEEE Trans. on Ind. Electron.*, vol. 65, no. 7, pp.5497-5508, 2018.

[21]   B. Li, J. Lu, W. Li, "Realization of CC and CV mode in IPT system based on the switching of double-sided LCC and LCC-S compensation network," *Int. Conf. Industrial Informatics Computing Technology, Intelligent Technology, Industrial Information Integration (ICIICII)*, pp. 364–367, 2016.

[22]   R. Mai; Y. Chen; Y. Li; Y. Zhang; G. Cao; Z. He, "Inductive power transfer for massive electric bicycles charging vased on hybrid topology switching with a single inverter," *IEEE Trans. Power Electron.*, vol. 32, no. 8, pp. 5897-5906, Aug. 2017.

[23]   L. Tan, S. Pan, C. Xu, C. Yan, H. Liu, and X. Huang, "Study of constant current-constant voltage output wireless charging system based on compound topologies," J. Power Electron., Vol. 17, No. 4, pp. 1109-1116, Jul. 2017.

[24]   H. Wang, H. Zhang and Y. Lei, "Analysis on wireless charging circuit characteristic under the hybrid compensation topology," *IEEE International Power Electronics and Motion Control Conference,* pp. 2450-2454, 2016.